Submitted to: SPIE 1992 International Symposium on Optical
Applied Science and Engineering
San Diego, CA July 19-24, 1992

BNL-47890
Conf-920792--32

An adaptive crystal bender for high power synchrotron radiation beams

Lonny E. Berman and J.B. Hastings
Brookhaven National Laboratory
National Synchrotron Light Source
Upton, New York 11973

BNL--47890

DE93 000376

ABSTRACT

Perfect crystal monochromators cannot diffract x-rays efficiently, nor transmit the high source brightness available at synchrotron radiation facilities, unless surface strains within the beam footprint are maintained within a few arcseconds. Insertion devices at existing synchrotron sources already produce x-ray power density levels that can induce surface slope errors of several arcseconds on silicon monochromator crystals at room temperature, no matter how well the crystal is cooled. The power density levels that will be produced by insertion devices at the third-generation sources will be as much as a factor of 100 higher still. One method of restoring ideal x-ray diffraction behavior, while coping with high power levels, involves adaptive compensation of the induced thermal strain field. The design and performance, using the X25 hybrid wiggler beam line at the National Synchrotron Light Source (NSLS), of a silicon crystal bender constructed for this purpose are described.

1. INTRODUCTION

Perfect crystal monochromators in synchrotron insertion device beam lines must be able to diffract x-rays efficiently, and faithfully preserve the brightness of the source, in the presence of adverse power loads. To do so, surface slope errors and dilations induced by the incident power must be maintained within the Darwin angular width of the crystal Bragg reflection used, commonly a few to several arcseconds, and certainly within the several arcsecond opening angle of the photon beam to avoid spoiling the source brightness. The x-ray power density levels at existing insertion device beam lines can already induce slope errors exceeding perfect crystal Darwin widths, and will increase by up to two orders of magnitude for such beam lines at the next generation of synchrotron sources now being constructed or commissioned. In addition to selecting the desired photon energy for use in an experiment, monochromator crystals are often aligned or figured to control beam polarization or harmonic content, x-ray bandwidth, divergence, or coherence, and for these applications, crystal distortions have to be kept within 10% of a Darwin width or smaller, the order of less than 1 arcsec. For these reasons, the proper functioning of perfect crystal optics in high power beam lines, the so-called "crystal cooling problem", is considered to be one of the foremost problems facing the users of the next generation of sources. This article addresses a pre-requisite to solving this problem: that of proper functioning of perfect crystal optics in existing high power beam lines. Solutions to this can then be extrapolated for use at future beam lines.

2. THE CRYSTAL COOLING PROBLEM

The crystal cooling problem can be separated into two components: removal of the power deposited in the crystal, and the thermal-elastic response of the crystal to the induced thermal strain field. The relative importance of the two can be evaluated in the present perspective by considering the power levels incident on the first crystal of the monochromator installed in a representative existing high power

*Work performed under the auspices of the U.S. Department of Energy, under contract DE-AC02-76CH00016.

beam line, the X25 27-pole hybrid wiggler beam line at the NSLS.[1] The X25 monochromator can be operated in one of two ways: unfocussed, whereby the direct wiggler beam (attenuated by graphite filters and a beryllium window) is incident on the first crystal, and focussed, whereby the direct beam is initially reflected off a double-focussing toroidal mirror upstream of the monochromator. In unfocussed running, the incident power can reach 350 W, spanning a cross-sectional area of 4 cm horizontal by 4 mm vertical (FWHM). This gives an average linear power density (integrated over the vertical) of about 9 W/mm, and a normal-incidence areal density of more than 2 W/mm^2. In focussed running, when the mirror is in place, the maximum incident power drops to about 100 W, but the cross-sectional area shrinks to 1.5 cm horizontal by 1.5 mm vertical, resulting in an average linear power density of 7 W/mm and an areal density of 4 W/mm^2. Insertion device beam line monochromators at other existing facilities are subjected to similar power loads, up to 3 times higher at the F2 beam line at the Cornell High Energy Synchrotron Source (CHESS).

These power and power density loads are modest enough that conventional convective cooling schemes using water suffice. The cooling methods in current use vary from indirect[1-3] (crystal thermally coupled to a water-cooled heat sink via a liquid metal, gas or other interface) to direct[4-7] (crystal directly water-cooled), and some take advantage of efficiency improvements such as jet-cooling[4,5] or enlarged contact area with coolant.[6,7] However all methods in regular use employ water as the coolant, and all, including the simplest ones, have sufficed to remove the deposited power from the crystal while preventing it from getting hot (e.g., to the point of melting, plastically deforming, or just giving unstable x-ray diffraction performance) and avoiding boiling of the coolant. Hence removal of the power deposited in the monochromator crystal is not worrisome at existing sources. It is felt, however, that for monochromators at the next generation of sources, some of which can expect to see 10 times higher powers and 100 times higher power densities, more sophisticated cooling techniques will have to be pursued in order to avoid problems such as coolant boiling or crystal deformation. Methods under investigation include the use of liquid gallium instead of water as a coolant for more efficient heat transfer,[8,9] and the use of porous cooled materials as heat sinks to dramatically enhance the cooling surface area.[10]

The thermal-elastic response of a crystal to the power load is an entirely different problem; insight into its magnitude can be gained through a simple one-dimensional heat flow calculation. Consider an unconstrained crystal wafer of thickness t, oriented at an incidence angle θ with respect to an x-ray beam of total power P, width W, and height H. If all of the power is absorbed at the top surface and the wafer is cooled from below, it will bend spherically to a radius R given by[8,11,12]

$$R = \frac{t}{\alpha \Delta T} = \frac{k}{\alpha} \times \left(\frac{P}{WH}\sin\theta\right)^{-1} \qquad (1)$$

where α is the thermal expansion coefficient of the crystal material, k is its thermal conductivity, and ΔT is the temperature difference between the top and bottom surfaces. In the plane of x-ray scattering, customarily the vertical, the integrated slope error $\Delta\theta$ across the beam footprint due to this thermal bowing is given by

$$\Delta\theta = \frac{L}{R} = \frac{H}{R\sin\theta} = \frac{\alpha}{k} \times \frac{P}{W} \qquad (2)$$

where $L = H/\sin\theta$ is the length of the beam footprint on the wafer surface in the scattering plane. Thus the slope error depends only on the material parameters α and k and the linear power density (integrated over the vertical) P/W, and not on

DISCLAIMER

the thickness t or incidence angle θ. For silicon wafers in the X25 monochromator, the calculated thermal slope error, using the 9 W/mm linear power density level and silicon's room-temperature values of 2.5×10^{-6} °C^{-1} for α and 0.15 W/mm°C for k, is 30 arcsec. The Darwin angular width of the Si(111) Bragg reflection, in comparison, is 9.6 arcsec at a photon energy of 6 keV and 4.5 arcsec at 12 keV. Hence the calculated thermal distortion is much higher than acceptable for ideal x-ray diffraction performance, even at existing insertion device beam lines, while the temperature gradient through the wafer is just 8.8°C/mm at 6 keV and 4.4°C/mm at 12 keV (for a beam power density of 4 W/mm^2). For germanium the problem gets worse. The calculated thermal strains using the much higher power densities anticipated at the next generation of sources reach the level where single crystals of silicon and germanium yield.[13]

In practice the crystal mounting may help to constrain it against bowing, so the observed thermal distortion can be much lower than calculated. The largest thermal distortions in the first crystal wafers used at X25, for instance, are less than 12 arcsec.[1] The wafer is floated on a 75:25 gallium:indium liquid eutectic layer spread over a water-cooled copper block.[2] The liquid layer is rather thin (several μm), and its surface tension may help to prevent bowing of the wafer. Also, the power load is rather anisotropic (footprint is much wider than its height), so the overall thermal bowing is cylindrical instead of spherical. More sophisticated crystal cooling methods usually involve complex mounting schemes, and care must be taken to minimize distortions arising from other sources, such as external[5] or coolant[6] pressure or bonding or clamping.[7] The observed mounting distortions in the X25 first crystal wafers are under 2 arcsec.[1]

Some techniques being pursued to minimize the thermal-elastic response problem aim at avoiding it altogether. At cryogenic temperatures, silicon's thermal conductivity becomes rather large and the thermal expansion coefficient goes to zero;[14] a recent experiment at X25[15] demonstrated that thermal slope errors in a liquid-nitrogen-cooled silicon crystal subjected to an exceptionally high power density level can be eliminated entirely. Another approach, which can be used at room temperature, is to incline the crystal in the horizontal plane to lower the linear power density P/W (which in addition reduces the thermal bowing component in the vertical scattering plane), while preserving a symmetric scattering geometry in the vertical plane; calculations[16,17] and measurements using the CHESS undulator[17] showed that this can also result in minimal thermal slope errors. Alternatively diamond, if available in perfect single crystal form, can be used instead of silicon at room temperature. Its thermal conductivity can be as much as 15 times higher than silicon's while its thermal expansion coefficient is half as much, yet its (111) Bragg reflection Darwin width is still 70% of silicon's (111) value; recent calculations[18] and measurements at X25[19] also showed that slope errors in the face of high x-ray power densities are minimal.

Other methods of dealing with the thermal-elastic response problem involve compensating for it. Thermal (tested with the CHESS undulator)[20] and mechanical (tested at X25)[13,21] methods of bending the silicon diffracting surface to compensate for the beam-induced thermal bowing distortion have been demonstrated successfully. The present thermal distortions in the X25 first crystal wafers are larger than acceptable for truly ideal behavior of the monochromator. This paper describes a modification of the floating silicon wafer mount in use at X25, to provide a means of bending the wafer to cancel the thermal bowing while maintaining a good thermal contact through the eutectic interface to the cooled heat sink.

3. CRYSTAL BENDER DESIGN

Figure 1 shows a photograph of the crystal bender. In actual use, the x-ray beam is incident from the right and diffracts toward the left. The silicon wafer is cut in the shape of an isosceles triangle, and its diffracting surface, facing upward in the photo, has a (111) orientation. It is constrained at its base via two stainless steel retainers, and an upward-directed force can be applied from below at the apex, generating a torque that causes the wafer to bend concave upward into a cylindrical shape.[22] The force is applied by a vacuum-compatible piezoelectric inchworm motor (Burleigh Instruments model IW-700), which has a single-step resolution of 5 nm and a travel range of 6.5 mm. This motor is identical to those already in use in the X25 monochromator for positioning the second crystal.[1] Beneath the wafer is a layer of liquid gallium-indium eutectic spread over a water-cooled copper block. In comparison with the eutectic layer normally used with the standard X25 first crystal, a generous amount of eutectic is used with this device, to ensure that the crystal continues to make contact with it as it is bent, and to prevent unwarranted resistance to bending due to high surface tension. Water flowing at a nominal rate of 4 l/min runs through a single 10 mm diameter channel across the middle of the copper block, parallel to the wafer's base and centered 9 mm below the top surface of the copper.

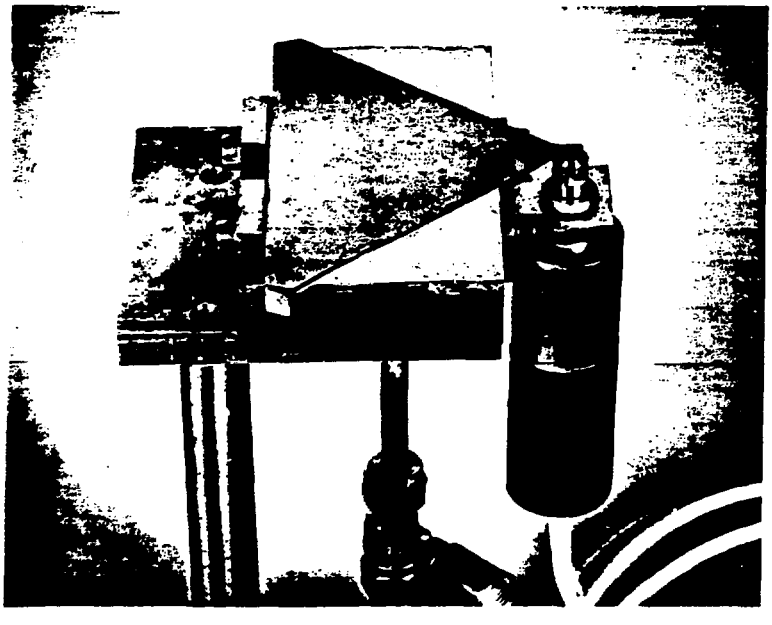

Fig. 1. Photograph of the crystal bender. The silicon wafer triangle has a base width of 9.5 cm and an altitude of 6 cm. The white x-ray beam enters from the right and diffracts toward the left.

The thin portion of the wafer triangle has a thickness of 0.8 mm, a base width of 9.5 cm and an altitude of 6 cm. Notice the thick region left across the base, of cross-section 6 mm by 6 mm. This feature was incorporated to prevent twisting of

the wafer along the direction parallel to the base, or across the horizontal extent of the x-ray beam, that might arise from the base constraint or bending. In practice, after the wafer is mounted, the screws that secure the two steel retainers are intentionally left loose. As the inchworm actuator expands and begins to contact the underside of the wafer, the whole crystal initially rotates until two opposite corners of the thick base region, the lower right and upper left edges, physically abut the copper block and steel retainers respectively, thus preventing further rotation of the base. Constraining the wafer in this manner guarantees a simple three-point contact and avoids distortions that can arise from clamping the retainers too tight. Thereafter, continued expansion of the actuator results in cylindrical bending of the thin silicon triangle. For a small actuator displacement D, the wafer bends to a radius R given by

$$R = \frac{A^2}{2D} \tag{3}$$

where A is the altitude of the wafer. Bending the wafer is this manner results in a mean rotation by an angle D/A in the x-ray scattering plane, causing the beam incidence angle to change by the same amount; to compensate for this, the entire device can be rotated in the opposite direction. A modification of the device, whereby the apex of the wafer triangle has a fixed elevation and the bending torque is produced via a rotation of the base,[23] would allow the mean incidence angle to remain unchanged as the wafer is bent.

4. EXPERIMENTAL SETUP

The x-ray diffraction characteristics of the bent silicon crystal were tested in the X25 experimental station under unfocussed white beam conditions, for which the experimenter can have direct access to the wiggler white beam (after transmission through two additional beryllium windows that terminate the beam line) in the hutch. The setup is shown in Fig. 2. The water-cooled bent first crystal and uncooled flat second silicon crystal are mounted on separate motorized high resolution rotation stages with single-step capabilities of 0.36 arcsec. The second crystal has the same (111) orientation as the first and serves as a perfect analyzer. By scanning its angle θ_2 while the first crystal angle θ_1 is held fixed, or vice versa, an x-ray double crystal rocking (reflectivity) curve profile of the Si(111) fundamental Bragg reflection can be measured using the ionization chamber D_1. By placing an appropriate filter in front of a second ionization chamber D_2, so as to suppress the fundamental reflection yet transmit the Si(333) harmonic at thrice the photon energy of the fundamental, a rocking curve profile for the intrinsically narrower harmonic could be measured simultaneously. The chosen photon energies for the tests were 6.17 keV for the Si(111) reflection and 18.51 keV for the Si(333) harmonic, corresponding to a Bragg angle θ_B of 18.7°. The theoretical rocking curve widths at these energies are 13 arcsec for Si(111) and 0.8 arcsec for Si(333). The broad width of the fundamental facilitated the initial alignment of the crystals, and the narrow width of the harmonic made it useful as a probe of thermal and mechanical strains.

For a fixed setting of θ_2 relative to θ_1, a topograph of the doubly-diffracted x-ray beam reveals the spatial distribution of diffracted intensity from the first crystal for a given Bragg angle, assuming the analyzer is perfect. By collecting topographs at different relative angle settings of the two crystals, a Bragg angle contour map of the illuminated region of the first crystal can be produced, giving information about the spatial distribution of slope errors and lattice dilations within this region. The fastest and simplest means of measuring an x-ray topograph is with film. Detailed analysis of the information

thus recorded then requires digitization of the image. In this and previous crystal cooling studies which we have undertaken,[1,5,13,21] the topographical information was directly recorded in digital form by scanning a 0.1 mm wide slit across the beam for each relative angle setting while simultaneously measuring the ionization chamber currents. For a white beam power variation, and consequently thermal strain profile, that are primarily along one direction (the vertical in Fig. 2),[1,5,21] the slit is set 0.1 mm wide, and scanned, only in this direction, thus producing a one-dimensional topograph; it is left wide open along the horizontal (which is perpendicular to the plane of Fig. 2). This was the case in the present study. For experiments in which the power, and thermal strain, profiles are two-dimensional,[13] the slit is made 0.1 mm wide both vertically and horizontally, and raster-scanned over both directions, producing two-dimensional topographs. The Bragg angle contours measured using the harmonic are more revealing than those using the fundamental, since the narrower rocking curve of the harmonic results in better contour resolution.

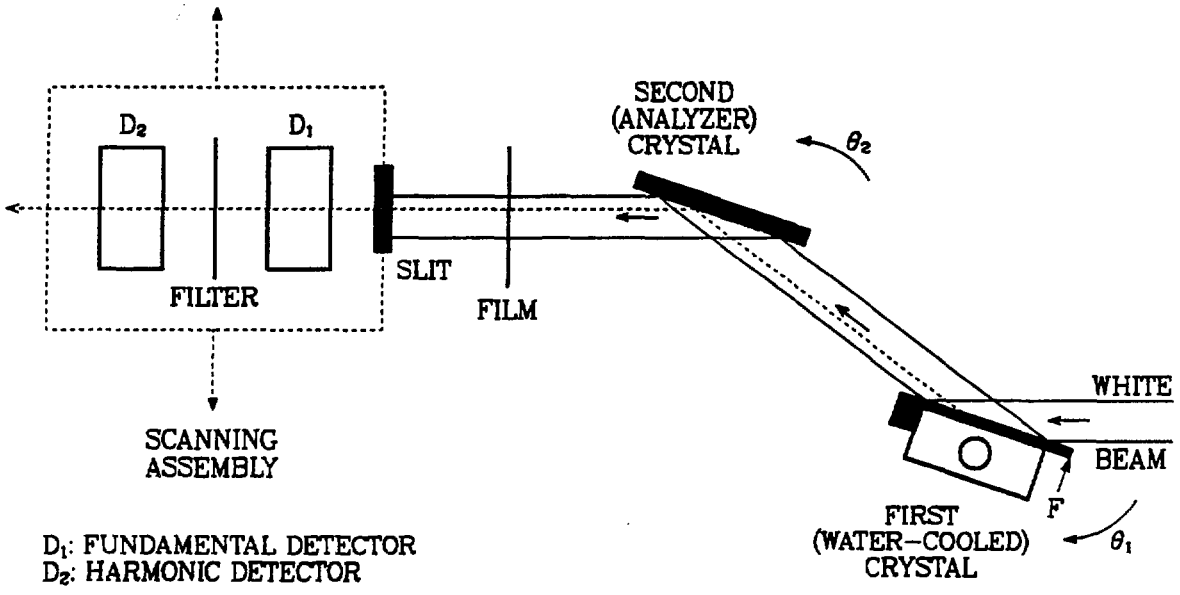

Fig. 2. Experimental setup for diagnosing thermal strains in the bent crystal, shown mounted on a copper block with internal water channel. The bending force F is applied with a piezoelectric inchworm actuator.

5. PRESENT MONOCHROMATOR BEHAVIOR AND NEED FOR COMPENSATION

To illustrate the problem which the crystal bender was designed to correct, consider the existing X25 floating-wafer monochromator. Figure 3 shows a set of Bragg angle topographs measured from the monochromator, as presently installed in the beam line.[1] Si(220) crystals were used, and the instrument was aligned at a 23.8° Bragg angle to diffract 8 keV in the fundamental and 16 keV in the (440) harmonic. The horizontal linear power density was 7 W/mm and the normal-incidence

areal density was just under 2 W/mm^2 for the measurement, with the synchrotron running conditions being 2.5 GeV beam energy, 175 mA current, and 1.1 T wiggler field. The vertically-scanning slit and detectors were located in the hutch, 9 m downstream from the monochromator. The solid and dashed curves in Fig. 3 represent the Si(440) contours, with adjacent contours separated by $\Delta\theta_2$ = 1 arcsec. Three (220) fundamental contours separated by $\Delta\theta_2$ = 5 arcsec are also shown. The movement of the contours with changing angle shows that different regions of the first crystal diffracted at different angles, and therefore the crystal's diffracting surface was not flat along the vertical extent of the beam footprint, or perhaps not of uniform lattice spacing.

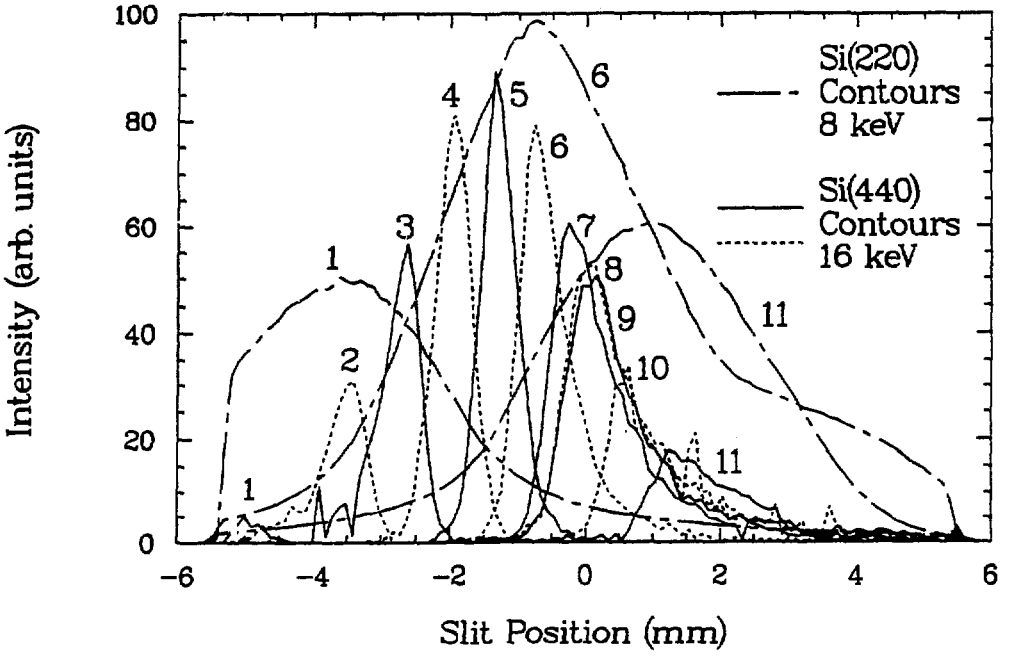

Fig. 3. Spatial distributions of diffracted intensity for the Si(220) fundamental and (440) harmonic reflections from the existing X25 beam line floating-wafer monochromator. The harmonic contours, labelled 1-11 and alternately represented as solid and dashed curves, are separated in angle by $\Delta\theta_2$ = 1 arcsec, with 1 the lowest and 11 the highest. The fundamental contours (chain-dashed) measured simultaneously with harmonic contours 1, 6, and 11 are also shown.

The advancement of contour position as the relative angle increases is indicative of an upwardly convex curvature of the first crystal surface. The curvature radius is determined by the rate of contour advance (in mm/arcsec) divided by $\sin\theta_B$. Near the beam center, where the power density was highest, the rate of advance is 0.6 mm/arcsec at the slit location, 27 m from the source, corresponding to 0.4 mm/arcsec at the monochromator, 18 m from the source (it is necessary to project the beam envelope back to its size at the monochromator to determine the true advance rate). This gives a curvature radius of 200 m in the vertical, i.e., the plane of Fig. 2. Using Eqn. 1, the expected thermal curvature for a free wafer

under these running conditions is about 100 m. Hence the crystal was flatter than expected, may be because of stiffening by the mount, or perhaps since the overall curvature was cylindrical instead of spherical (due to the anisotropic line-like incident power profile), requiring a scaling factor to be included in Eqn. 1. The crystal-thickness-dependent slope ("thermal bump") and lattice spacing variations along the vertical extent of the beam footprint,[8,11,12] arising from the non-uniform power profile across the incident white beam height, were expected to be much smaller than the thermal bowing slope errors under the running conditions in effect, since the floating wafer thickness was just 0.85 mm. A small lattice spacing variation along the beam footprint may explain the slight width variation of the contours.[5] The improved cooling of the crystal near the center of the beam (just above the water channel), where the power density was highest, compared with near the beam's top and bottom edges may have helped render the crystal's surface to be more isothermal, suppressing these lateral-profile-induced effects.[21]

It is the contour behavior displayed in Fig. 3 for which the new crystal bender is meant to correct. In the absence of thermal and mechanical strains, all the contours would be aligned (save for slight shifts due to beam steering), and have widths determined by the Gaussian opening angle of the incident photon beam; they would differ in intensity only, with the highest-intensity contour corresponding to the center of the rocking curve. Since the entire illuminated region of the first crystal does not contribute to the doubly-diffracted (440) flux for any given angle setting, the total flux is less than ideal at the center of the (440) rocking curve and greater than ideal in its wings. This, at the least, would make it difficult to eliminate the harmonic altogether through a slight angular misalignment between the two crystals. The throughput reduction problem is much smaller for the (220) reflection, and hence the device is still useful for the fundamental, but at higher photon energies the effect will be more pronounced since the Darwin angular width of total reflection gets smaller. The fundamental flux reduction will be obvious at all photon energies for the next-generation source power density levels. The crystal bender's main purpose is to compensate for any thermal curvature, flattening the crystal and hence restoring the ideal diffracted fundamental and harmonic fluxes through a double crystal monochromator at the centers of their respective rocking curves while sharpening the curves to their perfect profiles, allowing harmonic rejection via a relative angular misalignment to be feasible.

The first crystal's thermal curvature also further spreads the beam opening angle. The additionally divergent rays will diffract from the second crystal within the limit imposed by its Darwin width. Thus the parallelism of the x-ray beam gets smeared by up to the Darwin width of the Bragg reflection, reducing the beam brightness. The fundamental and harmonic rocking curves corresponding to the Fig. 3 contours had thermal broadening contributions of just under 8 arcsec,[7] larger than the (220) Darwin width of 5.2 arcsec at 8 keV. This is much less than the 40 arcsec opening angle of the X25 wiggler beam, but next-generation source opening angles are expected to be smaller. The crystal bender, when adjusted for proper thermal curvature compensation, will prevent the angular broadening of the photon beam and recover its full brightness. This would restore the utility of the instrument for applications involving multiple crystal tailoring of beam polarization,[24] divergence,[25] or coherence, for which small distortions of any of the component crystal elements cannot be tolerated. A first crystal bender installed in a synchrotron source double crystal monochromator has already been used to curve the crystal to follow the incident beam divergence in order to minimize the diffracted energy spread,[26] and the present bender can be used for this purpose as well.

6. CRYSTAL BENDER RESULTS

The recovery of the ideal rocking curve by the crystal bender is demonstrated in Fig. 4. The solid and chain-dashed profiles respectively represent the measured compensated and uncompensated rocking curves for (a) the Si(111) fundamental reflection at 6.17 keV and (b) the Si(333) harmonic at 18.51 keV. The entire experimental setup, including crystals and detectors, was contained within the X25 hutch as described earlier, with the scanning slit placed immediately downstream of the crystals. This avoids the beam projection and steering complications which needed to be accounted for in the analysis of the Bragg angle contours from the existing X25 monochromator just presented. The data shown in Fig. 4 were collected

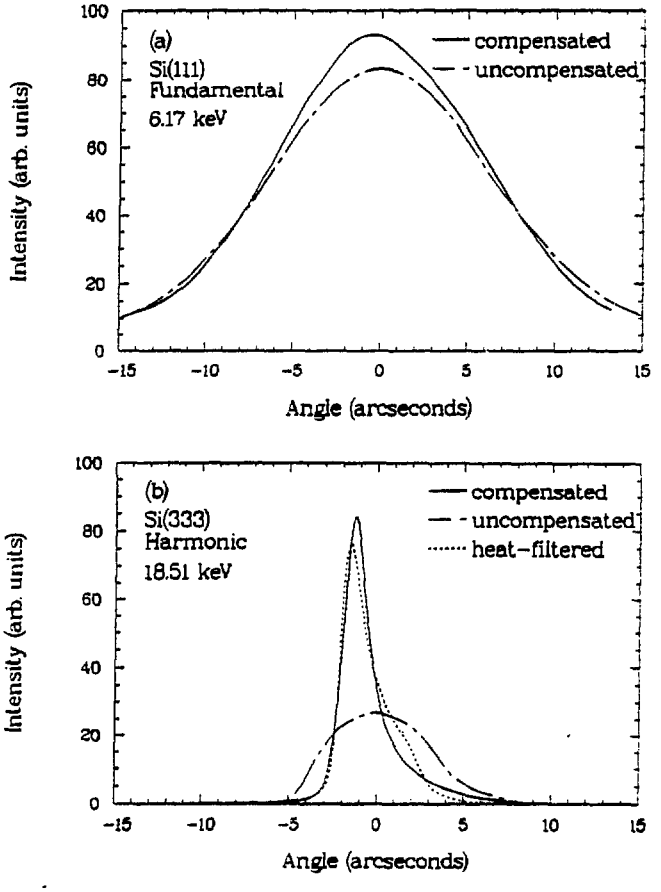

Fig. 4. Rocking curves measured from the triangular silicon wafer mounted on the crystal bender for (a) the (111) reflection at 6.17 keV and (b) the (333) reflection at 18.51 keV. The uncompensated curves were measured under high power with the wafer as mounted, and the compensated curves were measured after application of the optimum bending torque. The heat-filtered (333) curve was measured from the wafer as mounted under very low incident power.

at 105 mA machine current, with the incident beam, of cross-section 5 cm horizontal by 5 mm vertical (FWHM), having a total power of 125 W, horizontal linear density of 2.5 W/mm, and normal-incidence areal density of 0.5 W/mm^2. The uncompensated curves were associated with the triangular wafer as installed, prior to bending, and correspond to the free-floating configuration of the present X25 monochromator first crystal. The compensated curves were measured after bending the wafer with the inchworm motor to obtain the narrowest harmonic rocking curve, and show a modest peak intensity gain for the fundamental but a substantial gain for the harmonic.

The widths of the uncompensated rocking curves are 15.3 and 6.9 arcsec for the fundamental and harmonic respectively, improving to 14.3 and 1.9 arcsec for the compensated case. After moving the filter that is normally placed between the two ionization chambers into the path of the white beam, thereby reducing the incident power substantially, the dashed (333) rocking curve in Fig. 4b was measured with the wafer in the unbent condition (i.e., as mounted) in order to reveal the intrinsic mounting distortion. This curve has a width of 2.1 arcsec, and, after deconvoluting the theoretical 0.8 arcsec width, shows that the mounting strain contributed 1.9 arcsec. Hence mounting strain probably accounts also for the residual differences between the compensated "hot" crystal rocking curve widths and theory, however its effect may be slightly different with the wafer bent than with the wafer unbent. In any case the comparison shown in Fig. 4b confirms that the entire diffracted intensity loss and width broadening caused by the thermal distortion, and perhaps a bit resulting from the mounting distortion as well, can be recovered through proper adjustment of the bender.

A thermal broadening component of 6.6 arcsec was removed from the "hot" crystal harmonic rocking curve width upon compensation. The expected thermal broadening under the given conditions, using Eqn. (2), was 8.6 arcsec. An inherent resistance to bowing, due to the bender mount, may be responsible for the difference, however this is smaller than seen earlier for the free-floating wafer. In this respect, the triangular crystal, when supported kinematically in the bender, may be a better approximation to a free lamella, more readily responsive to the thermal stress and mechanical compensation.

Figure 5 shows a set of Bragg angle topographs of the bent crystal corresponding to the "hot" compensated rocking curves of Fig. 4. Six contours for both the (111) and (333) reflections are shown, with adjacent contours separated by $\Delta\theta_1$ = 0.72 arcsec. Taking into account that the free-floating wafer contours of Fig. 3 were measured under a higher power load, the improvement shown in Fig. 5 is still dramatic. The (111) contours overlap almost perfectly and span the full 6.17 keV beam envelope (of expected Gaussian FWHM height 6 mm), demonstrating perfect thermal distortion compensation for the fundamental; contours recorded at more extreme relative angles also did not shift in position. All of the (333) contours have some diffracted intensity across the full 18.51 keV envelope (of expected Gaussian FWHM height 4.5 mm) and are symmetric about the midpoint of the envelope (in stark contrast to the (440) contours of Fig. 3), indicating good compensation even at the level of the harmonic. The progression in harmonic contour profile, from a central peak on the low-angle side of the rocking curve up to contour 3 at the rocking curve center, to two symmetrically-displaced peaks on the high-angle side beginning with contour 4, may indicate that the compensated surface has a remanent s-shaped figure error within 0.72 arcsec.

Tests made at higher incident powers, up to 260 W (horizontal density 5 W/mm, normal-incidence areal density 1 W/mm^2, 220 mA machine current) gave similar results upon optimum adjustment of the bender. Under normal NSLS x-ray ring operations the

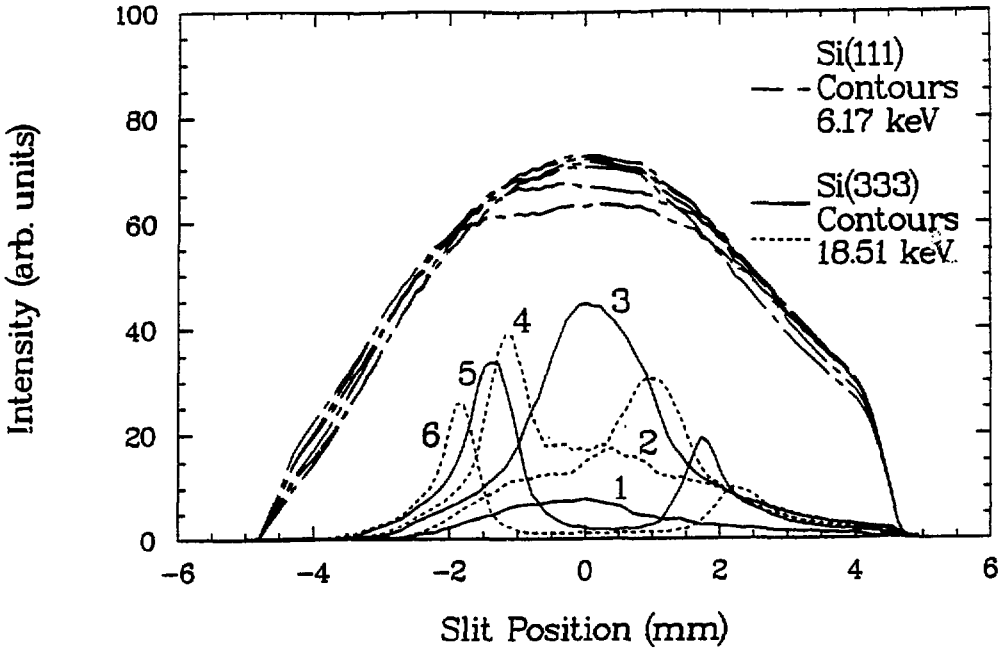

Fig. 5. Spatial distributions of diffracted intensity for the Si(111) fundamental and (333) harmonic reflections from the bent crystal under high power. The harmonic contours, labelled 1-6 and alternately represented as solid and dashed curves, are separated in angle by $\Delta\theta_1 = 0.72$ arcsec, with 1 the lowest and 6 the highest. The fundamental contours measured simultaneously are shown as chain-dashed curves.

machine current decays from 230 mA to 110 mA over a fill duration, usually lasting 24 hours. One method of using the bender under these conditions would be to vary the bend in a prescribed manner, dictated by the machine current variation. In the present design, Eqns. 2 and 3 show that this would give rise to a Bragg angle shift comparable to the thermal slope error change, since the length of the beam footprint L is a fraction of the wafer triangle altitude A. If we scale the results shown in Figs. 4 and 5 to the power levels at the X25 monochromator location, the thermal rocking curve broadening is expected to change from 18 arcsec at the beginning of an x-ray fill to 9 arcsec at the end, and continuous adjustment of the bender to compensate for this would cause a Bragg angle shift by a similar amount or higher. This shift can also be nulled in practice via rotation of the monochromator and adjustment of the second crystal. A simpler way to use the device would be to simply fix the compensating bend at the optimum level for the mid-fill current of 170 mA, obviating the need to perform any continuous adjustment. This would leave behind an uncompensated thermal distortion of 4.5 arcsec at the start- and end-points of the fill, which is much smaller than the time-averaged distortion experienced by the present instrument. It will improve further as the electron beam lifetime at the NSLS continues to improve, since this would result in raising the threshold current at which a fill is dumped, hence reducing the total power variation that the monochromator would encounter during the course of a fill.

7. SUMMARY

A simple crystal bender, designed to adaptively compensate the thermal distortion in a monochromator crystal exposed to a high power synchrotron radiation beam, has been constructed and tested successfully at the X25 hybrid wiggler beam line at the NSLS. It is capable of handling the power available at an existing insertion device beam line, and can completely null the induced thermal strain field, with concomitant recovery of the ideal transmitted flux and rocking curve profile for both fundamental and harmonic Bragg reflections to within the loss limit resulting from a small mounting strain of under 2 arcsec. Although its performance when subjected to third-generation source insertion device power levels has yet to be determined, there seems to be no reason why its design principles could not be incorporated in a similar instrument intended for a third-generation beam line monochromator, perhaps with modifications such as a thinner crystal or a more efficiently cooled heat sink so as to prevent too large of a temperature rise under the higher power densities. Projecting to the extremely high power densities expected at third-generation and beyond x-ray sources, adaptive compensation of thermal strains in monochromator and mirror optics may ultimately be required for all high- and low-resolution applications, even when using sensitivity-reducing approaches such as cryogenic cooling, glancing incidence geometries, or diamond as a substitute for silicon and germanium.

8. ACKNOWLEDGMENTS

We gratefully acknowledge discussions with and ideas from our colleagues Peter Siddons, Tom Oversluizen, Michael Hart and Sushil Sharma, and technical support from Anthony Lenhard and Gary Nintzel. This work was supported by the US Department of Energy under Contract No. DE-AC02-76CH00016.

9. REFERENCES

1. L.E. Berman, J.B. Hastings, T. Oversluizen, and M. Woodle, "Optical design and performance of the X25 hybrid wiggler beam line at the National Synchrotron Light Source", Rev. Sci. Instrum., Vol. 63, pp. 428-432, 1992.

2. D.H. Bilderback, D.M. Mills, B.W. Batterman, and C. Henderson, "The performance of a separated crystal x-ray monochromator during wiggler heating -- preliminary results", Nucl. Instrum. Methods Phys. Res., Sect. A, Vol. 246, pp. 428-433, 1986.

3. W. Schildkamp and D.H. Bilderback, "Helium cooling of x-ray optics during synchrotron heating", Nucl. Instrum. Methods Phys. Res., Sect. A, Vol. 246, pp. 437-439, 1986.

4. R. Cernik and M. Hart, "Medium power x-ray crystal optics for synchrotron radiation sources", Nucl. Instrum. Methods Phys. Res., Sect. A, Vol. 281, pp. 403-405, 1989.

5. L.E. Berman and M. Hart, "Performance of water jet cooled silicon monochromators on a multipole wiggler beam line at NSLS", Nucl. Instrum. Methods Phys. Res., Sect. A, Vol. 300, pp. 415-421, 1991.

6. T. Oversluizen, T. Matsushita, T. Ishikawa, P.M. Stefan, S. Sharma, and A. Mikuni, "Performance of a directly water-cooled silicon crystal for use in high-power synchrotron radiation applications", Rev. Sci. Instrum., Vol. 60, pp. 1493-1500, 1989.

7. J. Arthur, W.H. Tompkins, C. Troxel, Jr., R.J. Contolini, E. Schmitt, D.H. Bilderback, C. Henderson, J. White, and T. Settersten, "Microchannel water cooling of silicon x-ray monochromator crystals", Rev. Sci. Instrum., Vol. 63, pp. 433-436, 1992.

8. R.K. Smither, G.A. Forster, D.H. Bilderback, M. Bedzyk, K. Finkelstein, C. Henderson, J. White, L.E. Berman, P. Stefan, and T. Oversluizen, "Liquid gallium cooling of silicon crystals in high intensity photon beams", Rev. Sci. Instrum., Vol. 60, pp. 1486-1492, 1989.

9. R.K. Smither, W. Lee, A. Macrander, D. Mills, and S. Rogers, "Recent experiments with liquid gallium cooling of crystal diffraction optics", Rev. Sci. Instrum., Vol. 63, pp. 1746-1754, 1992.

10. T.M. Kuzay, "Cryogenic cooling of x-ray crystals using a porous matrix", Rev. Sci. Instrum., Vol. 63, pp. 468-472, 1992.

11. S. Joksch, D. Degenhardt, R. Frahm, G. Meyer, and W. Jark, "Heating effects of monochromator crystals at a high-intensity wiggler beam line", Nucl. Instrum. Methods Phys. Res., Sect. A, Vol. 291, pp. 325-333, 1990.

12. M. Hart, "X-ray monochromators for high-power synchrotron radiation sources", Nucl. Instrum. Methods Phys. Res., Sect. A, Vol. 297, pp. 306-311, 1990.

13. L.E. Berman, M. Hart, and S. Sharma, "Adaptive crystal optics for undulator beam lines", Nucl. Instrum. Methods Phys. Res., Sect. A, in press, 1992.

14. D.H. Bilderback, "The potential of cryogenic silicon and germanium x-ray monochromators for use with large synchrotron heat loads", Nucl. Instrum. Methods Phys. Res., Sect. A, Vol. 246, pp. 434-436, 1986.

15. G. Marot, M. Rossat, A. Freund, S. Joksch, H. Kawata, L. Zhang, E. Ziegler, L. Berman, D. Chapman, J.B. Hastings, and M. Iarocci, "Cryogenic cooling of monochromators", Rev. Sci. Instrum., Vol. 63, pp. 477-480, 1992.

16. J. Hrdý, "Double crystal monochromator for synchrotron radiation with decreased radiation power density", Rev. Sci. Instrum., Vol. 63, pp. 459-460, 1992.

17. A.M. Khounsary, "A novel monochromator for high heat load synchrotron x-radiation", Rev. Sci. Instrum., Vol. 63, pp. 461-464, 1992, and to be published, 1992.

18. S. Sharma, L.E. Berman, J.B. Hastings, and M. Hart, "Adaptive optics for high-power beam lines using diamond crystal monochromators", these Proceedings, 1992.

19. L.E. Berman, J.B. Hastings, D.P. Siddons, M. Koike, V. Stojanoff, and M. Hart, to be published, 1992.

20. R.K. Smither, "Variable focus crystal diffraction lens", Rev. Sci. Instrum., Vol. 60, pp. 2044-2047, 1989.

21. L.E. Berman and M. Hart, "Adaptive crystal optics for high-power synchrotron sources", Nucl. Instrum. Methods Phys. Res., Sect. A, Vol. 302, pp. 558-562, 1991.

22. M. Lemonnier, R. Fourme, F. Rousseaux, and R. Kahn, "X-ray curved-crystal monochromator system at the storage ring DCI", Nucl. Instrum. Methods, Vol. 152, pp. 173-177, 1978.

23. D.M. Mills, C. Henderson, and B.W. Batterman, "A fixed exit sagittal focussing monochromator utilizing bent single crystals", Nucl. Instrum. Methods Phys. Res., Sect. A, Vol. 246, pp. 356-359, 1986.

24. D.P. Siddons, M. Hart, Y. Amemiya, and J.B. Hastings, "X-ray optical activity and the Faraday effect in cobalt and its compounds", Phys. Rev. Lett., Vol. 64, pp. 1967-1970, 1990.

25. L.E. Berman, S.M. Durbin, and B.W. Batterman, "A channel-cut crystal monochromator for x-ray standing wave measurements", Nucl. Instrum. Methods Phys. Res., Sect. A, Vol. 241, pp. 295-301, 1985.

26. M.J. van der Hoek, W. Werner, and P. van Zuylen, "Design, construction and test results of a slitless, high-power, high-resolution double crystal x-ray monochromator for synchrotron radiation", Nucl. Instrum. Methods Phys. Res., Sect. A, Vol. 246, pp. 190-193, 1986.